Proceeding *20th SEAGC - 3rd AGSSEA Conference in conjunction with 22nd Annual Indonesian National Conference on Geotechnical Engineering.* Jakarta - INDONESIA, 6 -7 November 2018. ISBN No. 978-602-17221-6-9

Numerical Investigation of Wall Deflections Induced by Braced Excavations in Sands

Zhongjie Hou[2], Wengang Zhang*[12], Runhong Zhang[2], Wei Wang[2]
[1] *Key Laboratory of New Technology for Construction of Cities in Mountain Area, Chongqing University, Ministry of Education, Chongqing 400045, China*
[2] *School of Civil Engineering, Chongqing University, Chongqing 400045, China*
E-mail: cheungwg@126.com

ABSTRACT: Most previous studies focused on the performance of braced excavations in clays, where limited publications involved braced excavations in sands. In this study, to better understand the performance of braced excavations in sand, a series of two-dimensional (2D) and three-dimensional (3D) finite element analyses using the Hardening Soil (HS) model of PLAXIS software were performed to investigate the influences of soil properties, wall stiffness and excavation geometries, on the maximum wall deflection induced by braced-excavation in sand.. Results show that the maximum wall deflections calculated by 3D analysis are greater than those from 2D. Based on the numerical results, regression models were developed for estimating the maximum wall deflections induced by braced excavation in dense sand and medium dense sand, respectively.
Keywords: Braced excavation, wall deflection, sand, finite element analysis, Hardening Soil (HS) model, regression models

1. INTRODUCTION

Deep excavations are increasingly carried out in urban areas with development of underground space. However, the excavation process inevitably alters the stress states underground and may introduces significant wall deformations and ground movements, which would cause potential damage to the adjacent properties. To reduce the excavation-induced deformations, appropriate retaining walls and supporting systems should be designed through adequate construction methods. Based on the Nicoll highway collapse in Singapore and the Xianghu foundation pit accident in Hangzhou, China, an important design issue is to ensure the reliability of the structural systems, a common design criterion is to limit the maximum wall deflection to a fraction of the excavation depth He, typically in the range of 0.5~1.5%. However, most previous studies (Wong and Broms 1989, Kung et al. 2007, Wang et al. 2008, Xuan 2009, Hwang et al. 2012, Moh and Song 2013, Hsieh and Ou 2016, Zhang et al. 2015, Finno et al.2016, Goh et al. 2017) have investigated the behavior of wall affected by deep excavations in soft to stiff clays. There are only limited studies involving braced excavation in sands.

A number of researchers have adopted finite element method (FEM) to study the behavior of retaining systems in deep excavations. Nakai et al. (1999) conducted 2-D model test and the results were compared with FE analysis. It was found that the computed results describe well with the model test results. They also indicated that the stiffness of the wall, the wall friction, and the strut significantly influence the performance of the wall. Based on the back analysis using the MIT S1 soil model, Nikolinakou et al. (2011) analyzed excavations in Berlin sand and examined the structural systems and soil properties of the excavation. Khoiri and Ou (2013), Han et al. (2017) and Hsiung (2016) compared the FEM predicted results with measured data for some excavation case histories and validated the reliability of numerical analysis with HS model for predicting the wall deformations and ground settlements in sandy soils. Hsiung and Dao (2014) has made a comparison of the performance of three constitutive soil models, i.e. Morh-Coulomb model (MC model), Hardening soil model (HS model) and Hardening soil model with small-strain considerations (HSS model), in predicting excavation-induced wall deflection in sands. Results indicated that the HSS model and HS model perform better predictions than those of the MC model. Sabzi and Fakher (2015) studied the performance of buildings adjacent to excavation supported by inclined struts in sand soils, it was found that soil strength parameters (c and ϕ) significantly affect the horizontal wall displacement and the soil stiffness affects the ground surface settlement considerably.

As discussed previously, the performance of braced excavations in sand is still a hot topic due to limited research. The main purpose of this study is to study the behaviour of wall affected by deep excavations in sand based on extensive plane strain and 3D numerical analyses with HS models. The influences of soil properties, wall stiffness and excavation geometries on the maximum wall deflection induced by braced excavation in sand were investigated. Based on the numerical results, Logarithmic Regression (LR) models and Polynomial Regression (PR) models have been developed for estimating the maximum wall deflections induced by braced excavation in dense sand and medium dense sand, respectively.

2. NUMERICAL MODELLING

The FE software PLAXIS 2D (2017) and PLAXIS 3D (2017) were used to perform the excavation simulations. Figure 1 shows a typical cross-section and plan view for the cases considered. The embedded retaining wall together with a five-level strut system for He =17 m is also plotted in Figure 1. Relevant design parameters shown in the figure include: excavation lengths L of 36, 60 and 84 m, excavation widths B fixed at 30 m, excavation depths He of 17m, wall penetration depths into underlying stiff clay D of 5 m, thickness of sand layer T_1 and thickness of stiff clay layer T_2 of 25 and 30 m, respectively, horizontal strut spacing S_H of 4 and 5 m, and vertical strut spacing S_V of 3 m.

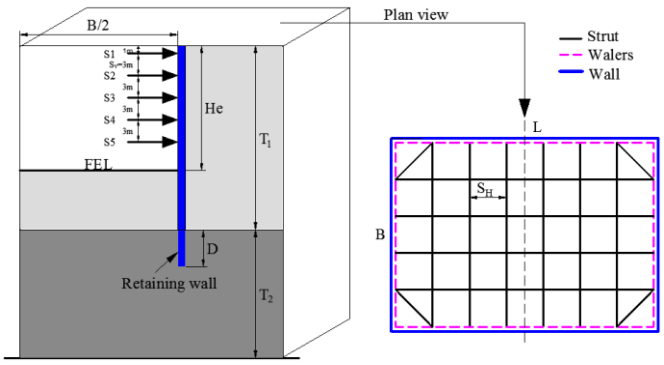

Figure 1 Cross-section and plan view of the numerical model

2.1 Numerical models

For 2D analysis, only half of the excavation model was developed due to symmetrical conditions for both the excavation sequence and geometry. A fine mesh size was adopted for 2D analysis to improve the accuracy of calculations. For 3D analysis, only a quarter mesh and a medium mesh size were used to reach a balance between accuracy and the processing time. Fig. 2 shows a typical 3D mesh plot, comprising of 93713 nodes and 63343 15-noded wedge elements.

Table 1 Wall properties for 2D and 3D analyses

Parameters		Wall types			
		flexible			medium
Plane strain (2D) FE parameters					
α		0.06	0.1	0.2	1.0
Wall stiffness *EI* (kNm^2/m)		3.224×10^4	5.407×10^4	1.081×10^5	5.407×10^5
Compressive stiffness *EA* (kN/m)		2205954	3.767×10^6	7.532×10^6	3.767×10^7
Poisson's ratio, *v*		0.15	0.15	0.15	0.15
Three-dimensional (3D) FE parameters					
Young's Modulus (kPa)	E_1	5.252×10^6	8.754×10^6	1.751×10^7	8.754×10^7
	E_2	2.626×10^5	4.377×10^5	8.754×10^5	4.377×10^6
Shear Modulus (kPa)	G_{12}	2.627×10^5	4.378×10^5	8.757×10^5	4.379×10^6
	G_{13}	8.754×10^5	1.459×10^6	2.918×10^6	1.459×10^7
	G_{23}	2.626×10^5	4.377×10^5	8.754×10^5	4.377×10^6
Poisson's ratio	*v*	0	0	0	0

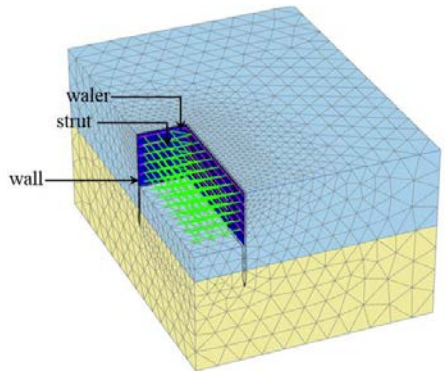

Figure 2 Typical quarter 3D mesh of excavation

In this study, the embedded retaining wall is simulated using 5-noded elastic plate elements for 2D analysis, while for 3D analysis, the wall is simulated using 8-noded quadrilateral plate elements with six degrees of freedom per node. Considering that the relatively flexible wall was generally designed and constructed for braced excavations in sands in engineering practice, two types of wall with four different stiffness values were considered for each soil type, as listed in Table 1. A stiffness coefficient α was utilized to represent walls with varying rigidities (Zapata-Medina and Bryson 2012). The baseline bending stiffness EI used to develop the different models was 540,675 kNm^2/m, which refers to a wall of medium stiffness based on databases of Long (2001) and Moormann (2012). Therefore, α=1.0 represents the cases with medium wall stiffness in this study. For flexible walls in sands, the baseline bending stiffness EI of 540,675 kNm^2/m was multiplied by smaller α values of 0.06, 0.1, and 0.2. Meanwhile, based on method adopted by Finno et al. (2016), the wall thickness of 0.42 m was set to be constant so that the moment of inertia I and area A of the plate were kept constant, and only elastic modulus E was varied. Besides, the soil-structure interactions are simulated through interfaces on both sides of the wall, which allow for the specification of a reduced friction between wall and the soil.

The shoring system of the braced excavation comprised of struts and walers. The struts were simulated via fixed end anchors in 2D analysis. For 3D analysis, beam elements were used to model the struts and walers, which have six degree of freedom per node. For the braced excavations considered in this study, the struts were designed horizontally at a regular spacing of 4 m in two directions to form a strong frame. The walers transfer the forces from the retaining wall to the struts and also stiffen and align the wall. The properties of shoring system are tabulated in Table 2.

Table 2 Properties of shoring system

Parameters		Struts	Walers
Young's Modulus *E* (kN/m^2)		2.1×10^8	2.1×10^8
Unit weight γ (kN/m^3)		78.5	78.5
Cross section area *A* (m^2)		0.007367	0.008682
Moment of inertia (m^4)	I_2	5.073×10^{-5}	3.668×10^{-4}
	I_3	5.073×10^{-5}	1.045×10^{-4}

The boundary conditions for the cases considered were: roller fixities at side boundaries to allow the vertical displacements; pinned at the bottom boundary to restrain any movements; the top boundary was free to move in all directions. For both 2D and 3D models, the lateral boundaries in the side directions were defined as 90 m away from the centre of the excavation to minimize the boundary effect of the mesh. The original ground water level inside the excavation was assumed at a depth of 5 m below the ground surface, which was progressively lowered with the excavation of the soil during each phase. Identical construction procedures of the simulation were applied as described in Table 3.

Table 3 Typical construction sequence for 2D analysis

Phases	Construction Details
Phase 1	Install the excavation wall
Phase 2	Excavate to 2 m below ground surface
Phase 3	Install strut system at 1 m below ground surface
Phase 4	Excavation to 5m below ground surface
Phase 5	Install strut system at 4 m below ground surface
Phase 6	Dewatering and excavation to 8 m below ground surface
Phase 7	Install strut system at 7 m below ground surface
Phase 8	Dewatering and excavation to 11 m below ground
Phase 9	Install strut system at 10 m below ground surface
Phase 10	Dewatering and excavation to 14 m below ground
Phase 11	Install strut system at 13 m below ground surface
Phase 12	Dewatering and excavation to 17 m below ground

2.2 Constitutive model and model parameters

The hardening-soil (HS) model was used to simulate the constitutive behavior of the two types of sands. This model involves frictional hardening characteristics to model plastic shear strain when subjected to primary deviatoric loading, and cap hardening to model plastic volumetric strain in primary compression. Failure is still defined by the M-C failure criteria. It should be noted that the hardening soil parameters of sands considered in this parametric study were based on the data extracted from Brinkgreve et al. (2010). The underlying stiff clay with average undrained shear strength cu = 125 kPa was based on the Gault clay found in Cambridge (Ng 1992). The HS parameters for different soils are summarized in Table 4.

Table 4 Hardening Soil parameters used for Finite-Element modelling

Hardening soil parameter Parameters	Unit	Medium dense sand (drained)	Dense sand (drained)	Stiff clay (undrained)
γ_{unsat}	kN/m^3	17	18.2	20
γ_{sat}	kN/m^3	19.8	20.3	20
$k_x=k_y=k_z$	m/day	1×10^{-8}	1×10^{-8}	1×10^{-8}
E_{50}^{ref}	kN/m^2	30000	48000	14847
E_{oed}^{ref}	kN/m^2	30000	48000	14847
E_{ur}^{ref}	kN/m^2	90000	144000	44540
c	kN/m^2	0	0	0.05
ϕ	°	34.3	38	33
Ψ	°	4.3	8	0
ν_{ur}	[-]	0.3	0.35	0.2
p^{ref}	kN/m^2	100	100	100
m	[-]	0.544	0.45	1
K_0^{nc}	[-]	0.436	0.384	0.455
R_f	[-]	0.938	0.9	0.96
R_{inter}	[-]	0.8	0.8	1

A series of FE simulations using Hardening Soil (HS) model were carried out to investigate the influences of soil properties, excavation geometries, wall stiffness α on the wall deflections induced by excavation. For brevity, the numerical results of the study are presented with the main findings, as described in the next sections.

3. FINITE ELEMENT ANALYSES

Figure 3 shows the typical wall deflection profiles corresponding to different excavation stages from 2D analyses in medium dense sand for wall stiffness α = 0.06 and 1.0. For the 3D rectangular braced excavation, only the profiles of the horizontal wall deflection at the centre of excavation are presented because the maximum lateral displacement occurs at this particular centreline location for symmetry. For brevity, only wall deflections caused by braced excavations in medium dense sand with L/B = 2.8 for α = 0.06 and 1.0 are plotted in Figure 4.

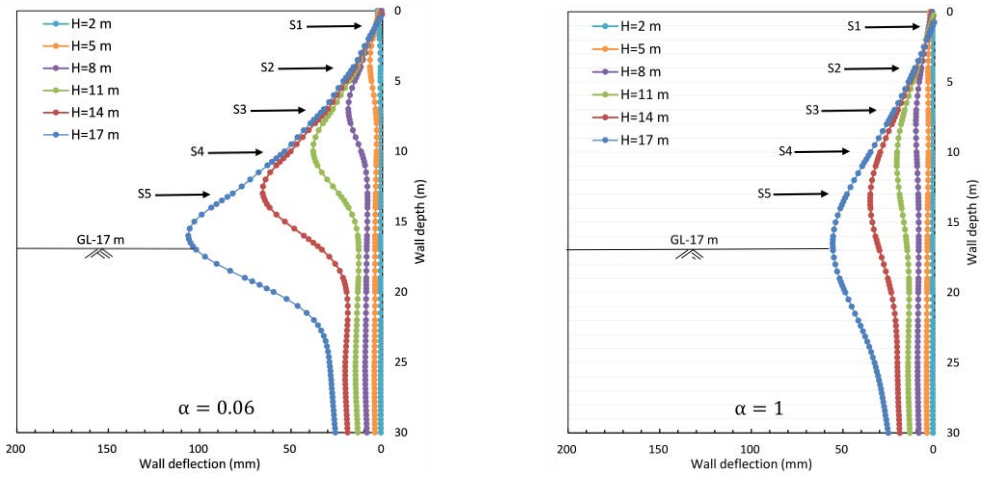

(a) α = 0.06 (b) α = 1.0

Figure 3 Wall deflection profiles for different excavation stages in medium dense sand from 2D analyses (α = 0.06,1.0)

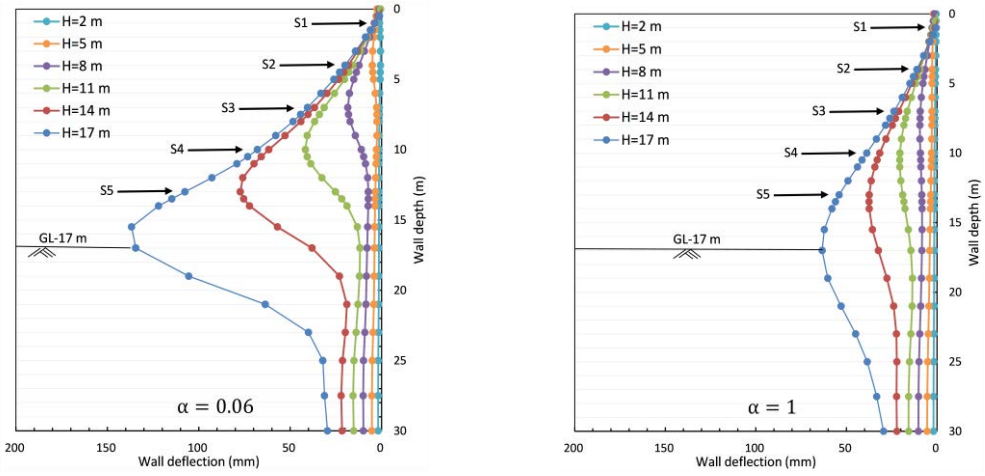

(a) α = 0.06 (b) α = 1.0

Figure 4 Wall deflection profiles for different excavation stages in medium dense sand from 3D analyses (α = 0.06,1.0)

Table 5 Typical maximum wall deflection for He = 17 m and α=0.06

Soil type	Excavation stage (m)	Maximum wall deflections (mm)							
		α = 0.06				α = 1			
		2D	3D			2D	3D		
			L/B = 1.2	*L/B* = 2.0	*L/B* =2.8		L/B = 1.2	*L/B* = 2.0	*L/B* =2.8
Medium dense sand	2	1.38	1.22	1.61	1.90	1.38	1.14	1.79	1.93
	5	4.36	5.05	4.89	5.31	4.36	3.30	5.02	5.46
	8	18.67	19.17	18.36	18.51	10.1	9.23	11.53	10.24
	11	37.91	45.89	43.15	41.71	20.5	20.75	20.25	20.58
	14	65.49	93.82	83.2	77.25	35.1	37.93	33.76	37.54
	17	106.2	192.4	149.7	136.7	55.5	64.73	54.34	63.44
Dense sand	2	0.78	1.04	1.53	1.81	0.8	1.26	1.55	1.84
	5	3.61	3.08	4.35	4.93	3.81	3.39	4.42	5.15
	8	7.60	9.17	8.83	9.13	7.81	6.40	8.28	9.52
	11	18.88	26.17	24.22	21.17	12.5	11.24	12.93	14.59
	14	35.05	55.61	48.55	42.85	18.9	21.40	21.53	21.08
	17	60.56	112.8	88.58	78.48	33.8	38.41	40.09	39.10

The distribution patterns of wall deflection profiles induced by excavations obtained from 2D simulations and 3D simulations are almost similar in shape, following a general trend that increasing wall stiffness leads to smaller maximum wall deflection in medium dense sand. The wall behaved in cantilever-mode first, and then changed to prop-mode after the struts were installed. The strut installation generally restrains the displacement of wall above the level of installed strut, especially for flexible and medium walls, so that the wall deflection profiles at various excavation stages almost coincide with each other above the installed struts. This agrees with the previous research by Hsiung et al. (2016). Generally, for the flexible walls, the wall deflection profile has a bulging shape with the maximum wall deflection between the excavation level and the toe of the wall.

For brevity, only some of the main results from 2D and 3D analyses are presented in Table 5. It can be found that the maximum wall deflection has a tendency to grow with the soil strength and decrease as the wall stiffness increases. Results in Table 5 also indicated that the wall displacements increase continuously as excavation proceeds. Generally, small horizontal displacement appears in the first two excavation stages, and becomes considerable in the subsequent stages. Maximum difference of wall deflection occurs in the last excavation stage, for medium dense sand, the maximum difference of wall deflections range from 93.82 mm to 192.4 mm in the final excavation stage for L/B=1.2 with wall stiffness α of 0.06.

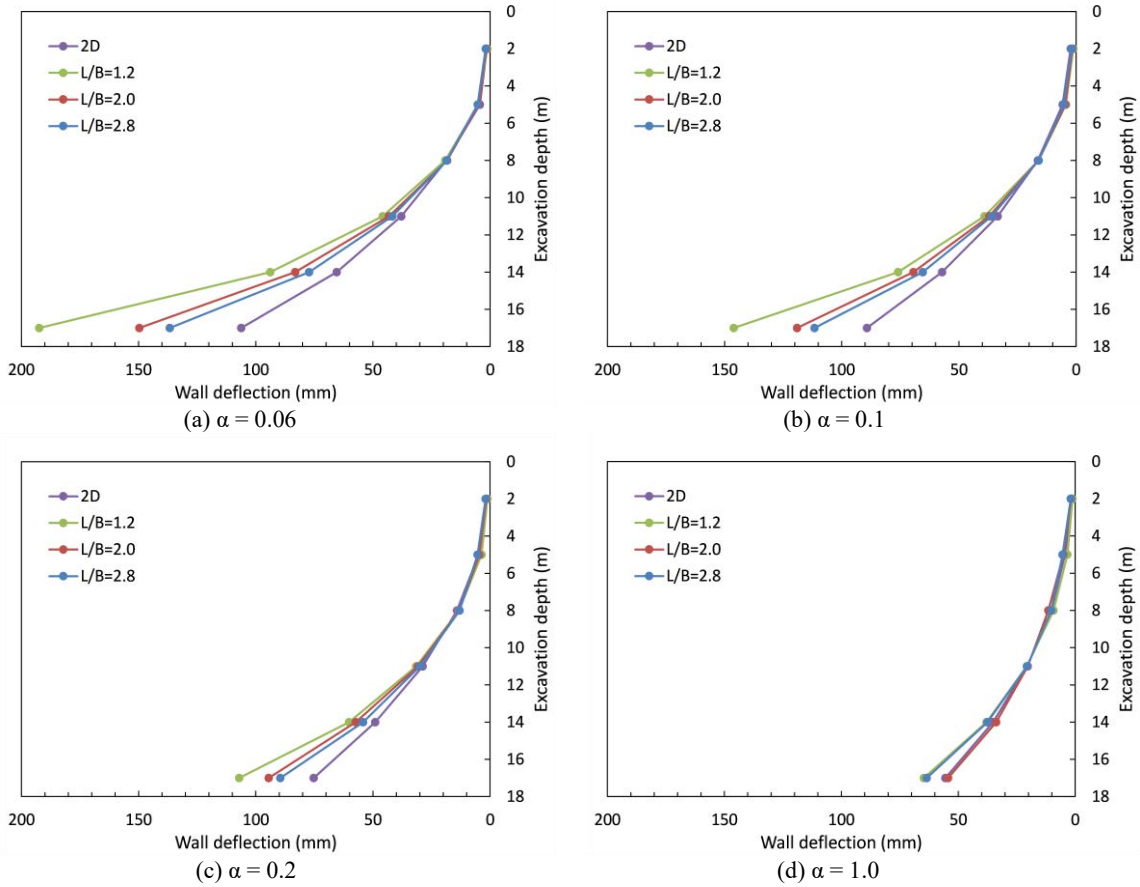

(a) α = 0.06 (b) α = 0.1

(c) α = 0.2 (d) α = 1.0

Figure 5 Maximum wall deflection for various *L/B* ratios in medium dense sand (α= 0.06, 0.1, 0.2 and 1.0)

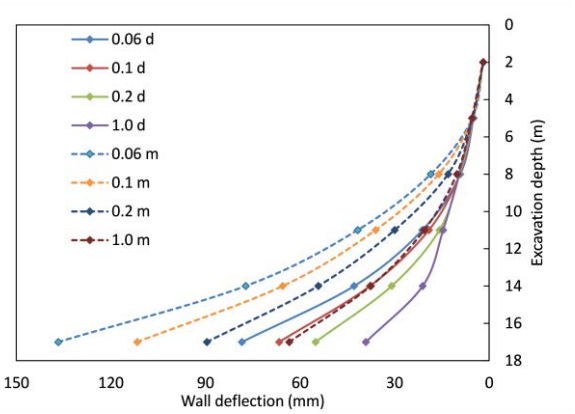

Figure 6 Maximum wall deflection for various excavation stage in two types of sands (d for dense sand while m for medium dense sand), L/B=2.8.

Figure 5 plots the maximum wall deflections of different excavation stages for various L/B ratios in medium dense sand (α= 0.06, 0.1, 0.2 and 1.0). In general, the horizontal wall displacements calculated by 3D simulations are greater than results from 2D simulations. It is also observed that for wall stiffness $\alpha \leqslant 0.2$, the wall deflection calculated by 3D simulations for various L/B ratios approximates to the results calculated by 2D simulations at excavation depth no more than 11 m, however, it has a tendency to grow with L/B ratios when excavation depth is more than 11 m below the ground level. Figure 6 compares the maximum wall deflections at various excavation stages with different wall stiffness in dense sand and medium dense sand for L/B=2.8. The observations show that the maximum wall deflection increases when soil strength decreases and decreases as the wall stiffness increases, similar to the trend described previously. It is evidently that the maximum wall deflection varies noticeably when excavation depth is greater than 5 m yet less difference when excavation depth is less than 5 m.

4. ESTIMATION MODELS

Based on the numerical results, Logarithmic Regression(LR) models and Polynomial Regression (PR) models have been developed for estimating the maximum wall deflection δ_{hm} induced by braced excavations in dense sand and medium dense sand, respectively. Four input parameters (S_v, L/B, α and He) are considered. For 2D numerical results, the optimal regression equation for wall deflection takes the following form:

$$\delta_h^* = a_0 S_v^{a1} (L/B)^{a2} \alpha^{a3} H_e^{a3} \quad (1)$$

For 3D results, the optimal regression equation takes the form of:

$$\delta_h^* = b_0 + b_1 S_v + b_2 S_v^2 + b_3 (L/B) + b_4 (L/B)^2 + b_5 \alpha + b_6 \alpha^2 + b_7 H_e + b_8 H_e^2 + b_9 S_v (L/B) + b_{10} S_v \alpha + b_{11} S_v H_e + b_{12} (L/B) \alpha + b_{12} (L/B) H_e + b_6 \alpha H_e \quad (2)$$

The values of the coefficients of Eq. (1) are shown in Table 6. Tables 7 and 8 tabulate the values of the coefficients of Eq. (2) for medium dense sand and dense sand, respectively.

Table 6 Coefficients for δ_h^*

Soil type	a_0	a_1	a_2	a_3
Medium dense sand	0.1896	0.36193	-0.18585	1.757
Dense sand	0.1067	0.2847	-0.09736	1.8802

Figure 7 shows the plot of the maximum wall deflection estimations using Eq. (1) versus the 2D FEM values, Eq. (1) is reasonably accurate with a high coefficient of determination R^2 of 0.9250 for medium dense sand and 0.9567 for dense sand, respectively. Similarly, Figure 8 shows the plot of the maximum wall deflection estimations using Eq. (2) versus the 3D FEM values, where there is a high coefficient of determination (R^2) of 0.9553 for medium dense sand and 0.9539 for dense sand, indicating the applicability and accuracy of the proposed Polynomial Regression (PR) models in predicting maximum wall deflections. It should be noted that there is a great scatter in points representing the LR model estimation against the FEM calculated results.

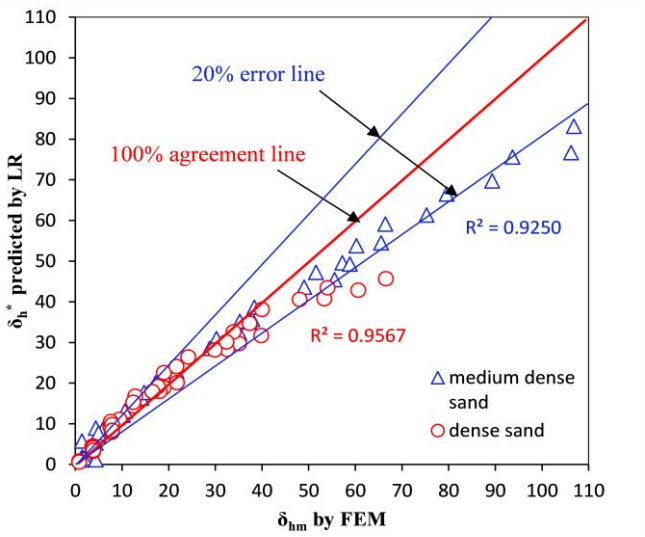

Figure 7 Predicted maximum wall deflection δ_h^* versus δ_{hm} by 2D FEM

Table 7 Coefficients for δh* in medium dense sand

b_0	b_1	b_2	b_3	b_4	b_5	b_6	b_7
0	4.484	0.8894	-109.593	-1.7618	-0.4462	1.4837	113.654
b_8	b_9	b_{10}	b_{11}	b_{12}	b_{13}	b_{14}	
0.6079	-0.6089	-0.8631	0.293	6.288	-1.0801	-5.2397	

Table 8 Coefficients for δ_{hm} in dense sand

b_0	b_1	b_2	b_3	b_4	b_5	b_6	b_7
0	4.1095	-1.6948	-59.823	-1.7105	-0.51504	1.0046	65.028
b_8	b_9	b_{10}	b_{11}	b_{12}	b_{13}	b_{14}	
0.38243	0.090104	-1.3302	0.2179	4.5105	-0.65509	-2.9924	

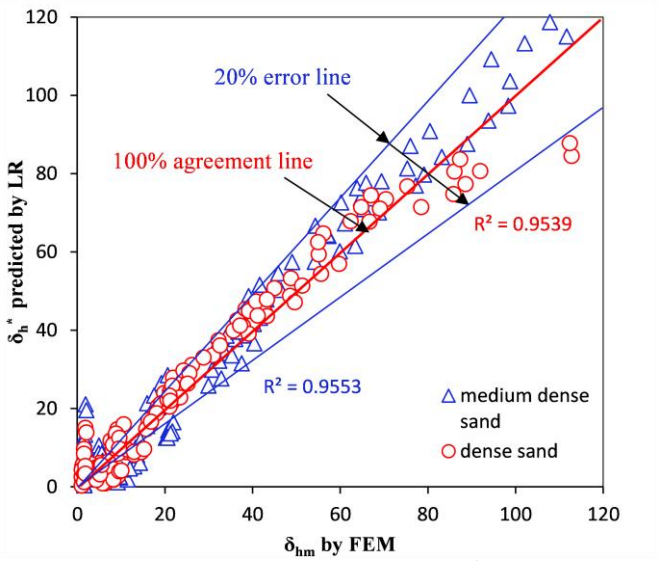

Figure 8 Predicted maximum wall deflection δ_h^* versus δ_{hm} by 3D FEM

5. SUMMARY AND CONCLUSIONS

In this study, a series of 2D and 3D simulations using the HS model for braced excavations in sands were carried out. In general, the horizontal wall displacements calculated by 3D simulations are greater than results from 2D simulations, the maximum wall deflection has a tendency to grow with soil strength and decreases as the wall stiffness increases. Meanwhile, it is found that small horizontal displacement appears in the first two excavation stages, and becomes considerable in the subsequent stages. On the other hand, based on the results, simple regression models are developed for estimating the maximum wall deflections induced by braced excavation in dense sands and medium dense sand, respectively. As shown in Eq.(1) and Eq.(2). These models relate the maximum wall deflection to various parameters including the vertical strut spacing S_v, L/B ratios, the wall stiffness α and excavation depth He, the high coefficient of determination (R2) indicates the applicability and accuracy of the proposed Polynomial Regression (PR) models in predicting maximum wall deflections.

6. REFERENCES

Brinkgreve, R., Engin, E., and Engin, H. K. (2010). "Validation of empirical formulas to derive model parameters for sands". In: Numerical Methods in Geotechnical Engineering, pp137–142.

Finno, R. J., Blackburn, J. T., and Roboski, J. F. (2016). "Three-dimensional effects for supported excavations in clay". Journal of Geotechnical and Geoenvironmental Engineering, 133(1), pp30-36.

Goh, A. T. C., Zhang, F., Zhang, W., and Chew, O. Y. S. (2017). "Assessment of strut forces for braced excavation in clays from numerical analysis and field measurements". Computers and Geotechnics, 86, pp141-149.

Han, J. Y., Zhao, W., Chen, Y., Jia, P. J., and Guan, Y. P. (2017). "Design analysis and observed performance of a tieback anchored pile wall in sand". Mathematical Problems in Engineering, 9, pp1-23.

Hsieh, P. G., Ou, C. Y. (2016). "Simplified approach to estimate the maximum wall deflection for deep excavations with cross walls in clay under the undrained condition". Acta Geotech; 11: pp177–89.

Hsiung, B. C. B., & Dao, S. D. (2014). "Evaluation of constitutive soil models for predicting movements caused by a deep excavation in sands". Electronic Journal of Geotechnical Engineering, 19, pp95-111.

Hsiung, B. C. B. (2016). "Impacts from three-dimensional effect on the wall deflection induced by a deep excavation in kaohsiung, taiwan". Japanese Geotechnical Society Special Publication, 2(45), pp1602-1607.

Hwang, R. N., Lee, T. Y., Chou, C. R., and Su, T. C. (2012). "Evaluation of performance of diaphragm walls by wall deflection paths". Journal of Geoengineering, 7(1), pp1-12.

Khoiri, M., & Ou, C. Y. (2013). "Evaluation of deformation parameter for deep excavation in sand through case histories". Computers and Geotechnics, 47(47), pp57-67.

Kung T. C., Juang C. H., Hsiao C. L. and Youssef M. A. H., (2007). "Simplified model for wall deflection and ground-surface settlement caused by braced excavation in clays". Journal of Geotechnical and Geoenvironmental Engineering, ASCE, 133(6), pp731-747.

Long, M. (2001). "Database for retaining wall and ground movements due to deep excavations". Journal of Geotechnical and Geoenvironmental Engineering, 127(3), pp203-224.

Moormann, C. (2012). "Analysis of wall and ground movements due to deep excavations in soft soil based on a new worldwide database". Soils and Foundations -Tokyo-, 44(1), pp87-98.

Moh, Z. C., and Song, T. F. (2013). "Performance of diaphragm walls in deep foundation excavations". In: First International conferences on case histories in geotechnical engineering, Missouri University of Science and Technology; pp1335–43.

Nakai, T., Kawano H., Murata K., Banno M., and Hashimoto T. (1999). "Model Tests and Numerical Simulation of Braced Excavation in Sandy Ground: Influences of Construction History, Wall Friction, Wall Stiffness, Strut Position and Strut Stiffness". Soils and Foundations, 39 (3): pp1–12.

Ng, C.W.W. 1992. "An Evaluation of Soil-Structure Interaction Associated with a Multi-propped Excavation". Ph.D thesis, University of Bristol, U.K.

Nikolinakou, M. A., Whittle, A. J., Savidis, S., & Schran, U. (2011). "Prediction and interpretation of the performance of a deep excavation in berlin sand". Journal of Geotechnical and Geoenvironmental Engineering, 137(11), pp1047-1061.

Sabzi, Z., and Fakher, A. (2015). "The performance of buildings adjacent to excavation supported by inclined struts". International Journal of Civil Engineering, 13(1), pp1-13.

Wang, I. W., Teng, F. C., Seed, R. B., and Ou, C. Y. (2008). "Using buttress walls to reduce excavation-induced movements". Geotechnical Engineering, 161(4), pp209-222.

Wong K. S, and Broms B. B. (1989). "Lateral wall defections of braced excavations in clay = déplacements latéraux des parois d'excavations avec butons dans l'argile". Journal of Geotechnical Engineering.

Xuan F. (2009). "Behavior of diaphragm walls in clays and reliability analysis". M.Eng.Thesis, Nanyang Technological University, Singapore.

Zapata-Medina, D. G., & Bryson, L. S. (2012). "Method for estimating system stiffness for excavation support walls". Journal o`f Geotechnical & Geoenvironmental Engineering, 138(9), pp1104-1115.

Zhang, W., Goh, A. T. C., and Xuan, F. (2015). "A simple prediction model for wall deflection caused by braced excavation in clays". Computers and Geotechnics, 63, pp67-72.